

## Role of microstructure and layer thickness in porous silicon conductometric gas sensors

Z. Gaburro<sup>\*1</sup>, C. J. Oton<sup>1,2</sup>, M. Ghulinyan<sup>1</sup>, L. Pancheri<sup>1</sup>, L. Pavese<sup>1</sup>, and N. Capuj<sup>2</sup>

<sup>1</sup> INFN and Dipartimento di Fisica, University of Trento, 38050 Povo (TN), Italy

<sup>2</sup> Departamento de Física Básica, University of La Laguna, 38204 La Laguna, Tenerife, Spain

Received 1 March 2004, revised 3 September 2004, accepted 27 January 2005

Published online 27 May 2005

PACS 07.07.Df, 73.61.Cw, 81.05.Rm

The electrical injection in porous silicon fabricated with heavily doped p-type silicon is very sensitive to NO<sub>2</sub>. The known effect is an injection increase associated to NO<sub>2</sub>. We show experimentally a strong correlation between two structural properties and the sensitivity of electrical injection to NO<sub>2</sub>. The first property is the microstructure, i.e. the pore morphology at nm scale. A structure with straight, elongated pores shows large sensitivity, as opposed to a branching structure. The second property is the layer thickness, which determines the sign of the effect of NO<sub>2</sub>. If the thickness is sufficiently low – of the order of few μm – the injection in presence of NO<sub>2</sub> decreases, instead of increasing.

© 2005 WILEY-VCH Verlag GmbH & Co. KGaA, Weinheim

### 1 Introduction

Porous Si (pSi) is fabricated by anodization of bulk Si wafers using HF based solutions [1]. Its internal surface to volume ratio can be several hundreds m<sup>2</sup> per cm<sup>3</sup>, leading to strong dependence of optical and electrical properties of pSi on the environment [2–7]. For this reason, pSi is an interesting material for gas and vapour sensors [8]. An intriguing case is the DC electrical response of pSi to gaseous nitrogen dioxide (NO<sub>2</sub>). NO<sub>2</sub> is a well known air pollutant originated by internal combustion engines and causing lung diseases. It is known that the current injection in metal/pSi/Si diodes biased at constant voltage dramatically increases when exposed to controlled flux of air containing NO<sub>2</sub>. The increase can reach one order of magnitude at NO<sub>2</sub> concentrations of the order of 100 ppb [9–12]. Such level of sensitivity is exceptionally high for solid state sensors working at room temperature, and opens the way to potential applications: in fact, the warning level of NO<sub>2</sub> for human health is set right to about 100 ppb by pollution regulations worldwide.

Known facts about the injection increase in pSi associated to exposure to NO<sub>2</sub> can be summarized as follows. The effect is best observed in mesoporous Si (mpSi), fabricated from heavily B-doped p-type (p<sup>+</sup>) substrates, i.e. whose resistivity  $\rho$  is in the mΩ cm range; moreover, experimental reports deal with thick mpSi samples (at least some tens of μm), and whose porosity ranges between 50% and 80% [9–13]. The injection increase is due to an increase of free carriers (holes) associated to the presence of NO<sub>2</sub>, as directly evidenced by free-carrier absorption characterization with FTIR apparatus on thick, contactless mpSi layers [13]. The sensitivity of injection is very large because mpSi samples are essentially depleted of free carriers, even though the concentration of dopants (B) is not significantly altered by the anodization of the p<sup>+</sup> substrates [14]. It is argued that the carrier depletion without removal of the dopants is a consequence of the anodization process: the anodization develops most effectively breaking Si–Si rather than Si–B bonds, thus preferentially proceeding around – and avoiding removal of – B

\* Corresponding author: e-mail: gaburro@science.unitn.it, Phone: +39 0461 882054, Fax: +39 0461 881696

dopants. As a consequence, in the leftover p<sup>+</sup>Si skeleton, B dopants tend to be located at – or at close distance from – the surface, where the concentration of defect states is large. Defect states trap free holes, effectively inhibiting the acceptor function of B dopants, and resulting in the remarkably low conductivity of mpSi [13, 14]. It has been also suggested that mobility is also lower in mpSi [13], although without general agreement [15]. The increase of hole concentration associated to the exposure to NO<sub>2</sub> indicates that the acceptor function of B dopants must be in some sense “re-activated” by NO<sub>2</sub> [11, 13]. In order to understand how this “reactivation” is functioning, one can investigate its dependence on fabrication parameters. For example, the correlation between sensitivity and porosity has been already investigated [9]. However, a physical picture of the connection between porosity and sensitivity is difficult. Samples with very different specific surface or structure might have the same porosity, and yet they should be expected to exhibit different sensitivity. In this work we address this question, looking for structural characteristics of highly sensitive samples. We demonstrate that the sensitivity is highly depending on two structural properties of mpSi, one in the microscopic scale (the pore shape) and the other in macroscopic scale (the mpSi layer thickness).

## 2 Experimental procedures

p<sup>+</sup>Si layers were fabricated by electrochemical dissolution in an HF-based solution using single-crystalline p-type ⟨100⟩ heavily-doped Si substrates. Substrate nominal resistivity  $\rho$  was 6–15 m $\Omega$  cm. Before anodization, the native oxide was removed from the backside of the wafers, and aluminium back contacts were deposited by evaporation. The anodizing solution was obtained by mixing aqueous HF (48% wt.) with ethanol. We have tested different solutions, introducing small variations in the final nominal concentration of HF, which was ranging between 12% and 13% in volume. As expected, lower (higher) HF concentration led to higher (lower) porosity samples [1]. The etching was performed by applying an etching current density of 50 mA/cm<sup>2</sup>. After anodization, the samples were rinsed in ethanol and pentane, and dried in ambient air. Scanning Electron Microscopy (SEM) images were used to evaluate the porous layer thickness. Normal reflectance was measured to evaluate the refractive index  $n$  of the samples from interference figure. The porosity was extracted from the value of  $n$  by using Bruggeman approximation. Gold electrodes were deposited by evaporation on the mpSi top surface. Copper wires were connected to the gold electrodes using an epoxy silver paste. For the electrical characterization, the sensors were kept in a sealed chamber under controlled flux of gases coming from certified cylinders. Humid air was obtained by flowing dry air through a bubbler. Different relative humidity levels and NO<sub>2</sub> concentrations were obtained by mixing humid air, dry air and a dilute solution of NO<sub>2</sub> in air (550 ppb) with a computer driven flow control system. Relative humidity was monitored using a calibrated hygrometer.

## 3 Results and discussion

### 3.1 Role of microstructure

We compare the response of two thick samples, which were fabricated by using the same procedure except for the concentration of HF of the electrochemical solution. In the following, the two samples, fabricated with [HF] = 12% and 13%, are referred to as Sample A and B, respectively. The porosity of Sample A and B was, respectively, 78% and 60%. Top view Transmission Electron Microscopy (TEM) images and the effect of exposure to NO<sub>2</sub> (at 50 ppb concentration) under three humidity conditions (at 30%, 0% and 70% relative humidity) are shown in Fig. 1.

In Fig. 1, no injection change is observed in the 60% porosity sensor (Sample B) under exposure to NO<sub>2</sub> (50 ppb), as opposed to the 78% porosity sensor (Sample A). At the HF concentration and the current density of this work (respectively, 12%–13% and 50 mA/cm<sup>2</sup>), the anodization is close to the electropolishing regime [1]. At 12% concentration, in particular, the anodization becomes very aggressive because of its closeness to electropolishing regime. This can be seen in Fig. 1 (Sample A), where several B dopants have been removed. In fact, the B density of these samples ( $N_B \approx 10^{19}$  cm<sup>-3</sup>) would imply the presence of about 1 ion every 2 or 3 nm along any linear direction, whereas Sample A has empty

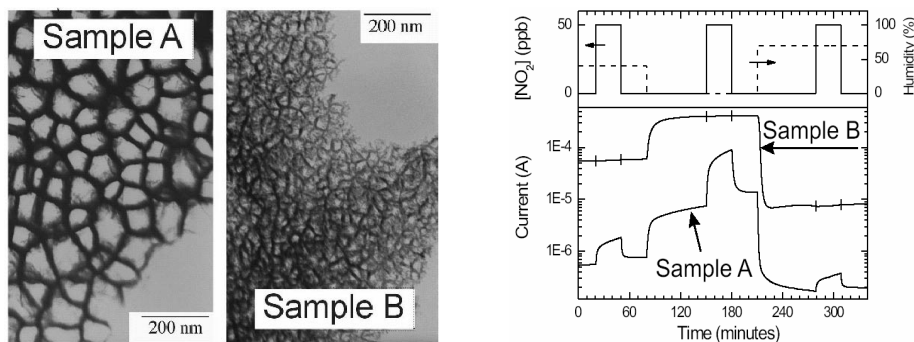


**Fig. 1** Left: TEM images of top view (100 plane) of two porous silicon samples. Sample A: porosity (extracted from reflectance) = 78%, thickness = 32.5  $\mu\text{m}$ . Sample B: porosity (extracted from reflectance) = 60%, thickness = 37.2  $\mu\text{m}$ . Right: simultaneous measurement of electrical conduction of Samples A and B under controlled atmosphere. The top graph shows the composition of the gas. Solid line:  $\text{NO}_2$  concentration, either 0 or 50 ppb, left axis. Dashed line: relative humidity (40%, 0 or 70%, right axis). Bottom graph: electrical current under DC constant voltage bias (1 V) between the top gold electrode and the p+ substrate, during exposure to gas.

gaps of several tens of nm. The closeness of the electropolishing threshold also implies significant structural differences associate to small changes in the solutions: a mild increase of the HF concentration to 13% restores the expected progression of the anodization described in the Introduction, which leaves the B dopants in the porous skeleton [14] (Fig. 1, TEM of Sample B).

In order to discuss the different sensing behaviour shown in the right panel of Fig. 1, one should first notice that, from the porosity difference, the amount of leftover Si in Sample A (78% porosity) is about two times less than in Sample B (60% porosity). However, the resistance is 2 orders of magnitude larger in Sample A. A second observation is that a structural difference is apparent by comparing the TEM images. The Si structures of Sample B are more branching and interconnecting with each other than those of Sample A. This is confirmed both by side-views TEM images of pore walls (not shown), and by light scattering experiments on Sample A (experimental data shown elsewhere [16]). The peculiar light scattering of Sample A is not observed in Sample B, and is originated by the straight pore walls of Sample A [16], i.e. it is a consequence of the microstructure. We propose the following connection between microstructure and sensitivity. The resistors of Fig. 2 represent local resistance along pore

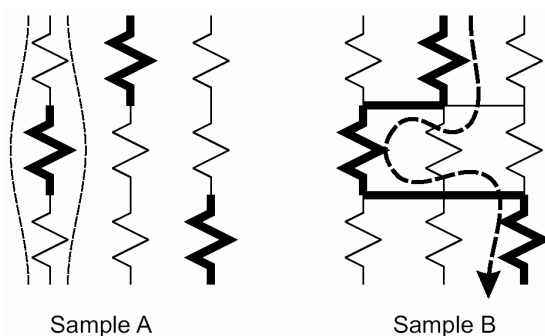


**Fig. 2** Schematic interpretation of resistive paths of samples shown in Fig. 1. Larger (smaller) resistance is represented by thin (thick) resistors. In Sample A, paths are less interconnected, and high resistors represent the conduction bottleneck. Local increases of resistance can be due, for example, to wall narrowing (undulating shape, thin dashed lines at left side of Sample A) and/or to higher dopant inhibition. In the more interconnected mesh (Sample B), high resistors are more likely to be bypassed. The selection of a dominating low resistance path is emphasized by a dashed line with arrow.

walls. Pore walls of Sample A are less interconnected, thus high resistance portions are less likely to have local bypasses with lower resistance. Therefore, high resistivity paths dominate in the total Sample A resistance. The highly resistive pore walls are the most sensitive to  $\text{NO}_2$ , since thinner walls have larger fraction of dopants at close distance from the surface.  $\text{NO}_2$  locally reactivates the acceptor dopant, thus reverting the high resistivity to lower resistivity paths. In the case of Sample B, the presence of bypasses, whose resistance is low even in absence of  $\text{NO}_2$ , obscures the effect of  $\text{NO}_2$ . This interpretation qualitatively agrees with both the large difference of resistance in absence of  $\text{NO}_2$ , and the difference of sensitivity to  $\text{NO}_2$ .

### 3.2 Role of thickness

We compare the response of a thick sample and a thin sample. They were fabricated by using the same procedure (HF concentration was 12% in both cases), except for the anodization time, which was, respectively, 1363 and 127 s, for the thick (32  $\mu\text{m}$ ) sensor and the thin (2  $\mu\text{m}$ ) sensor. The experimental data of electrical injection in presence of  $\text{NO}_2$  are reported in Fig. 3, which clearly shows the *opposite* variation in the two sensors.

The opposite behavior of the two sensors most likely results from the competition of two opposite effects of  $\text{NO}_2$  on the injection. The injection-enhancing effect is known, and it is due to hole detrapping, as described in the Introduction. A model which can provide also an injection-inhibiting effect of  $\text{NO}_2$  has been proposed by Boarino et al. [11]. In mpSi, close the midgap energy, there is a high density of dangling bonds ( $D_0$ ). Even though the B dopants ionize, such defect states inhibit the freeing of holes by supplying electrons to B ( $\text{B}_3^0 + D^0 \leftrightarrow \text{B}_4^- + D^+$  [11]). Therefore, defect states work as hole traps at the surface. The “B reactivation” in presence of  $\text{NO}_2$  is due to band-bending (Fig. 3b) [11]. The relevant feature of this model is the energetically favorable location of holes at the outer surface of conductive paths. The pulling to the surface is a reduction of the effective conductive area (Fig. 3b), or, more appropriately, of the hole mobility, because of the larger scattering in proximity of the surface. Thus, the effect of  $\text{NO}_2$  is twofold: holes are de-trapped and pulled at the surface. In thin sensors, the injection-inhibiting mechanism dominates because the free-hole population is significant even in absence of  $\text{NO}_2$ , whose enhancing-effect has therefore little impact onto the injection. This can be seen by observing that (in absence of  $\text{NO}_2$ ) the current injection is three orders of magnitude larger in thin than in the thick sensors (Fig. 3, left panel). The hole density in thin sensors is large everywhere, because the junctions are close to each

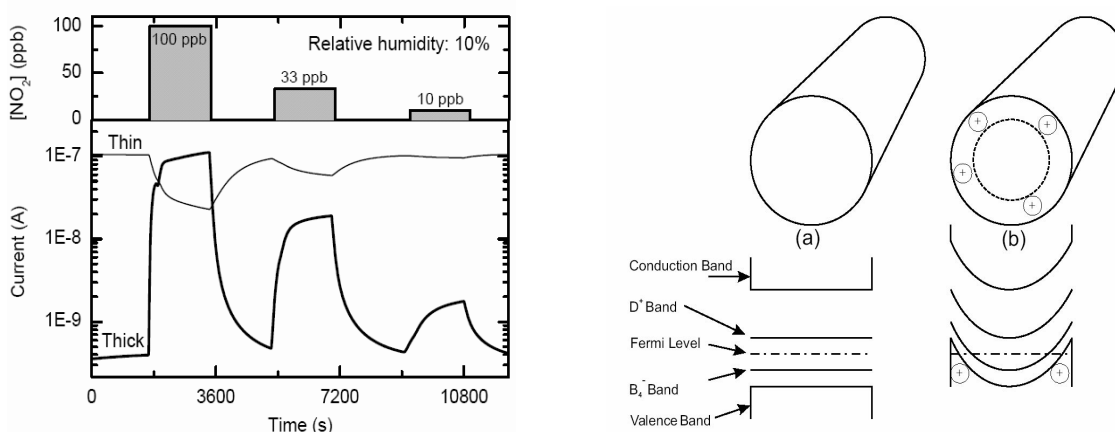


**Fig. 3** Left: simultaneous measurement of current injection in thick and thin sensors, under fixed bias voltage (bottom plot) and under controlled gas flux as a function of time. The bias voltage was 1 V. The top plot shows the composition of the gas flux. Right: pictorial representations of a conductive path of porous Si, in absence (a) and in presence (b) of  $\text{NO}_2$ . The energy states of each case are qualitatively shown underneath.

other, and the whole mpSi layer is flooded of holes diffusing from the junctions. This flooding requires that the thickness of mpSi is 2  $\mu\text{m}$  or less, as resulting from similar considerations on  $n^+/i/n^+$  structures [17].

## 4 Conclusions

The main effect of  $\text{NO}_2$  on mesoporous silicon is to increase the free hole density. However, when the mpSi microstructure is highly branching and the electrical paths are heavily interconnecting each other in random directions, there is large probability of establishing preferential electrical paths through thicker, insensitive branches. Thus, sensitivity of the electrical injection to  $\text{NO}_2$  is highly quenched. There is also an injection-inhibiting effect of  $\text{NO}_2$ , due to upward band-bending at the surface. This latter effect is equivalent to a narrowing of the conductive cross-sections, or more appropriately to a lowering of the effective hole mobility due to larger scattering of carriers with the surface. In thin sensors, this latter effect dominates because the free hole density is high even in the absence of  $\text{NO}_2$ . On the contrary, in thick sensors, the dominating effect remains the increase in free hole density. As a consequence, the net effect of  $\text{NO}_2$  in thick and thin porous silicon sensors is opposite in sign.

**Acknowledgements** We acknowledge the support of INFM, progetto PAIS 2001 “SMOG” and of Provincia Autonoma di Trento. C. O. acknowledges a fellowship granted by Cajacanarias and University of La Laguna.

## References

- [1] For recent general reviews of porous Si see for example A. G. Cullis, L. T. Canham, and P. D. J. Calcott, *J. Appl. Phys.* **82**, 910 (1997).  
O. Bisi, S. Ossicini, and L. Pavesi, *Surf. Sci. Rep.* **38**, 1 (2000).
- [2] V. M. Demidovich, G. B. Demidovich, E. Dobrenkova, and S. Kozlov, *Sov. Tech. Phys. Lett.* **18**, 459 (1992).
- [3] M. Ben-Chorin, A. Kux, and I. Schechter, *Appl. Phys. Lett.* **64**, 481 (1994).
- [4] D. Stievenard and D. Deresmes, *Appl. Phys. Lett.* **67**, 1570 (1995).
- [5] V. S. Y. Lin, K. Motesharei, K. P. S. Dancil, M. J. Sailor, and M. R. Ghadiri, *Science* **278**, 840 (1997).
- [6] S. Zangoie, R. Jansoon, and H. Arwin, *J. Vac. Sci. Technol. A* **16**, 2901 (1998).
- [7] P. A. Snow, E. K. Squire, P. St. J. Russel, and L. T. Canham, *J. Appl. Phys.* **86**, 1781 (1999).
- [8] M. J. Sailor, in: *Properties of Porous Silicon*, edited by L. Canham (IEE Inspec, London, U.K., 1997), p. 364.
- [9] L. Boarino, C. Baratto, F. Geobaldo, G. Amato, E. Comini, A. M. Rossi, G. Faglia, G. Lerondel, and G. Sberveglieri, *Mater. Sci. Eng. B* **69–70**, 210 (2000).
- [10] C. Baratto, G. Faglia, G. Sberveglieri, L. Boarino, A. M. Rossi, and G. Amato, *Thin Solid Films* **391**, 261 (2001).
- [11] L. Boarino, F. Geobaldo, S. Borini, A. M. Rossi, P. Rivolo, M. Rocchia, E. Garrone, and G. Amato, *Phys. Rev. B* **64**, 205308 (2001).
- [12] L. Pancheri, C. J. Oton, Z. Gaburro, G. Soncini, and L. Pavesi, *Sens. Actuators B* **89**, 237 (2003).
- [13] V. Y. Timoshenko, T. Dittrich, V. Lysenko, M. G. Lisachenko, and F. Koch, *Phys. Rev. B* **64**, 085314 (2001).
- [14] G. Polisski, G. Dollinger, A. Bergmaier, D. Kovalev, H. Heckler, and F. Koch, *phys. stat. sol. (a)* **168**, R1 (1998).  
G. Polisski, D. Kovalev, G. Dollinger, T. Sulima, and F. Koch, *Physica B* **263–274**, 951 (1999).
- [15] E. Garrone, S. Borini, P. Rivolo, L. Boarino, F. Geobaldo, and G. Amato, *phys. stat. sol. (a)* **197**, 103 (2003).
- [16] C. J. Oton, Z. Gaburro, M. Ghulinyan, L. Pancheri, P. Bettotti, L. Dal Negro, and L. Pavesi, *Appl. Phys. Lett.* **81**, 4919 (2002).  
C. J. Oton, M. Ghulinyan, Z. Gaburro, P. Bettotti, L. Pavesi, L. Pancheri, S. Gialanella, and N. E. Capuj, *J. Appl. Phys.* **94**, 6334–6340 (2003).
- [17] V. Cech, *J. Appl. Phys.* **88**, 5374 (2000).